MOLECULAR DYNAMICS SIMULATIONS OF THE ELASTIC MODULI OF POLYMER-CARBON NANOTUBE COMPOSITES

Michael Griebel and Jan Hamaekers

Department of Applied Mathematics, University of Bonn, Wegelerstr. 6, D-53115 Bonn, Germany.

1 Introduction

Very long pure carbon tube-like structures were first reported by Iijima in 1991.[1] These nanotubes (*NT*) can be used to reinforce polymer composites. Because the bending stiffness of NTs is in the range of 0.4–$4\,\mathrm{TPa}$,[2] they possess the potential for large increases in strength and stiffness when compared to typical carbon-fiber-reinforced polymer composites. In this work, we derive stress-strain curves from molecular dynamics (*MD*) simulations of polyethylene (*PE*) NT composites to predict their macroscopic elastic moduli and compare them to the rule-of-mixtures.
In several earlier works, MD simulations have been successfully applied to predict elastic properties of PE/NT composites.[3,4] So far, the application of strain has been accomplished by uniformly expanding the length of the simulation cell and the coordinates of the atoms in the direction of the deformation. Then, a MD simulation or a potential energy minimization is performed to equilibrate the system and to measure the corresponding stress. In the present work, we carry out the application of strain by employing a Parrinello-Rahman-Nosé Lagrangian to control stress and temperature.[5,6] We compute the stress-strain curves of three periodic model-systems, an infinite $(10,10)$ carbon NT, a capped $(10,10)$ carbon NT embedded in PE, and the PE matrix itself. To model the bonded interaction within these hydrocarbon systems, we use a many-body bond order potential (*REBO*) due to Brenner[7] with an additional van der Waals term[8] (*model I*). Alternatively, we model the PE matrix by a united-atom potential[9] and just the NT by Brenner's potential (*model II*). In both models, the nonbonded interaction of the atoms is represented by a Lennard-Jones potential. We exploit the slopes of the stress-strain curves to derive different elastic moduli and constants.

2 Computational Methods

To obtain an isothermal-isobaric ensemble (*NPT*), we introduce additional degrees of freedom to an N-particle constant volume and constant energy ensemble (*NVE*) with cartesian coordinates $\vec{x}_i$, masses m_i and a potential V. We define a time-dependent matrix $\hat{h} = [\vec{a}_1, \vec{a}_2, \vec{a}_3]$ consisting of the basis vectors of the simulation cell and re-scale the coordinates $\hat{\vec{s}}_i = \hat{h}^{-1}\vec{x}_i$. We also re-scale the time t by $\bar{t} = \int_0^t \gamma(\tau)d\tau$ and obtain the velocities in the form $\dot{\vec{x}}_i(\bar{t}) = \gamma\hat{h}\dot{\hat{\vec{s}}}_i(t)$. Then, we define the fictitious potentials $P_{\mathrm{ext}} \det\hat{h}$ and $N_f k_B T \ln\gamma$ with the external pressure P_{ext} and the target temperature T, the system's number of degrees of freedom N_f and Boltzmann's constant k_B. Now a so-called Parrinello-Rahman-Nosé Lagrangian can be postulated and an extended Hamiltonian

$$\mathcal{H} = \frac{1}{2}\sum_{i=1}^{N}\frac{\vec{p}_{\vec{s}_i}^{\,T} G \vec{p}_{\vec{s}_i}}{m_i} + \frac{1}{2}\frac{\mathrm{tr}(p_h^T p_h)}{M_P} + \frac{1}{2}\frac{p_\gamma^2}{M_T} + V(h, h\vec{s}_1, \ldots, h\vec{s}_N) + P_{\mathrm{ext}}\det h + N_f k_B T\eta \tag{1}$$

with variables $\vec{s}_i(t) := \hat{\vec{s}}_i(\bar{t})$, $h(t) := \hat{h}(\bar{t})$, $G := h^T h$, and $\eta(t) := \ln\gamma(\bar{t})$, can be derived.[5,6,10] Here, M_P and M_T are fictitious masses. The resulting equations of motion (*EQM*) read as

$$\dot{\vec{s}}_i = \frac{\vec{p}_{\vec{s}_i}}{m_i}, \quad \dot{h} = \frac{p_h}{M_P}, \quad \dot{\eta} = \frac{p_\gamma}{M_T}, \tag{2}$$

$$\dot{\vec{p}}_{\vec{s}_i} = -h^{-1}\nabla_{\vec{x}_i}V - G^{-1}\dot{G}p_{\vec{s}_i} - \frac{p_\gamma}{M_T}p_{\vec{s}_i}, \tag{3}$$

$$\dot{p}_h = \left(\Pi_{\mathrm{int}} - \mathrm{diag}\,(P_{\mathrm{ext}})\right)h^{-T}\det h - \frac{p_\gamma}{M_T}p_h, \tag{4}$$

$$\dot{p}_\gamma = \sum_{i=1}^{N}\frac{\vec{p}_{\vec{s}_i}^{\,T} G \vec{p}_{\vec{s}_i}}{m_i} + \frac{\mathrm{tr}(p_h^T p_h)}{M_P} - N_f k_B T. \tag{5}$$

Here, the internal stress tensor Π_{int} can be written as

$$\Pi_{\mathrm{int}} = \frac{1}{\det h}\left(\sum_{i=1}^{N} m_i h\vec{s}_i\vec{s}_i^{\,T}h^T - \frac{d}{d\,h}V\right)h^T. \tag{6}$$

To accomplish various tensile load cases, we use an additional external stress tensor Π_{ext} within the EQM (4)

$$\dot{p}_h = \left(\Pi_{\mathrm{int}} - \mathrm{diag}\,(P_{\mathrm{ext}}) + \Pi_{\mathrm{ext}}\right)h^{-T}\det h - \frac{p_\gamma}{M_T}p_h. \tag{7}$$

Additionally, we apply a constraint to get a symmetric displacement matrix $e = hh^{-1}_{\mathrm{equilibrated}} - 1$, which then equals the *linear strain tensor* ε.
For the numerical solution of the system of the ordinary differential equations (2)-(5), we employ the "predictor-corrector" time integration scheme based on Beeman's approach[11] and later modified by Refson[12], to solve the difficulty of the velocity-dependent forces in the EQM (2)-(5).

3 Numerical Experiments

All tensile load tests are carried out at *normal conditions*, i.e. for $T = 273.15\,\mathrm{K}$ and for $P_{\mathrm{ext}} = 1.01325 \cdot 10^{-4}\,\mathrm{GPa}$. The fictitious masses are set to $M_T = 10.0\,\mathrm{u\,\AA}^2$ and $M_P = 10.0\,\mathrm{u}$. We use a timestep of $0.1\,\mathrm{fs}$ for model I and $0.2\,\mathrm{fs}$ for model II. We use a stress rate of $0.01\,\mathrm{GPa/ps}$ in all tensile load test cases and measure the induced stress $\pi := -\Pi_{\mathrm{int}}$ and strain ε. Details of the studied systems are given in figure 1 and the derived elastic constants are summarized in tables 1-3.

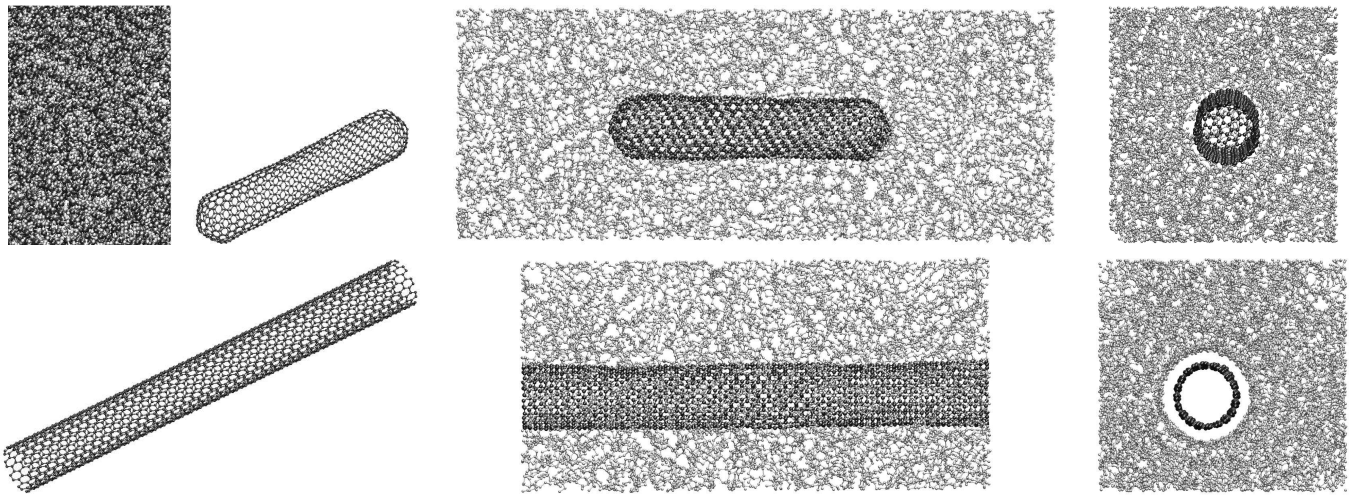

Fig. 1: We studied the following systems: (a) A PE matrix containing 9 chains of 1330 CH_2 units. (b) A $6\,\mathrm{nm}$ capped $(10,10)$ NT embedded in 8 chains of 1420 CH_2 units. Each of the NT caps consists of one half C_{240} molecule. (c) A periodically replicated $(10,10)$ NT spanning the length of the unit cell embedded in 8 chains of 1095 CH_2 units. In all equilibrated systems the PE matrix has a density of approximately $0.9\,\mathrm{g/cm^3}$. The volume fraction of the NT is approximately 2.8% for (b), and approximately 6.5% for (c). Additionally, we computed a Young's modulus of $403.85\,\mathrm{GPa}$ and a Poisson ratio a of 0.23 for the NT of system (c). Note that all materials are assumed to be *orthotropic*, thus the compliance matrix has only nine independent constants. The nanotubes are aligned parallel with the third coordinate direction.

$$\frac{1}{0.85}\begin{pmatrix} 0.77 & -0.34 & -0.44 & 0.0 & 0.0 & 0.0 \\ & 0.80 & -0.45 & 0.0 & 0.0 & 0.0 \\ & & 1.00 & 0.0 & 0.0 & 0.0 \\ & & & 2.54 & 0.0 & 0.0 \\ & & \mathrm{sym} & & 3.71 & 0.0 \\ & & & & & 3.22 \end{pmatrix} \approx \frac{1}{\tilde{E}}\begin{pmatrix} 1 & -\tilde{\nu} & -\tilde{\nu} & 0.0 & 0.0 & 0.0 \\ & 1 & -\tilde{\nu} & 0.0 & 0.0 & 0.0 \\ & & 1 & 0.0 & 0.0 & 0.0 \\ & & & 2(1+\tilde{\nu}) & 0.0 & .0.0 \\ & & \mathrm{sym} & & 2(1+\tilde{\nu}) & 0.0 \\ & & & & & 2(1+\tilde{\nu}) \end{pmatrix}$$

Tab. 1: The computed compliance matrix of (a) model II has nearly isotropic form; right hand side with modulus $\tilde{E} := E_{33}^{\mathrm{a,II}} \approx 0.85$ and ratio $\tilde{\nu} := (\nu_{11,33}^{\mathrm{a,II}} + \nu_{22,33}^{\mathrm{a,II}})/2 \approx 0.44$; see table 3. Here, we used the stress-strain relation $(\varepsilon_{11}, \varepsilon_{22}, 2\varepsilon_{33}, 2\varepsilon_{12}, 2\varepsilon_{23})^T = S(\pi_{11}, \pi_{22}, \pi_{33}, \pi_{12}, \pi_{23})^T$ to compute the components of the compliance matrix S.

System	S	C
(b)	$\begin{pmatrix} 1.24 & -0.62 & -0.21 & 0.0 & 0.0 & 0.0 \\ & 1.27 & -0.18 & 0.0 & 0.0 & 0.0 \\ & & 0.57 & 0.0 & 0.0 & 0.0 \\ & & & 3.43 & 0.0 & 0.0 \\ & & \mathrm{sym} & & 5.27 & 0.0 \\ & & & & & 5.88 \end{pmatrix}$	$\begin{pmatrix} 1.29 & 0.73 & 0.71 & 0.0 & 0.0 & 0.0 \\ & 1.24 & 0.67 & 0.0 & 0.0 & 0.0 \\ & & 2.22 & 0.0 & 0.0 & 0.0 \\ & & & 0.29 & 0.0 & 0.0 \\ & & \mathrm{sym} & & 0.19 & 0.0 \\ & & & & & 0.17 \end{pmatrix}$
(c)	$\begin{pmatrix} 1.013 & -0.351 & -0.0087 & 0.0 & 0.0 & 0.0 \\ & 0.869 & -0.0085 & 0.0 & 0.0 & 0.0 \\ & & 0.0393 & 0.0 & 0.0 & 0.0 \\ & & & 2.83 & 0.0 & 0.0 \\ & & \mathrm{sym} & & 7.47 & 0.0 \\ & & & & & 5.94 \end{pmatrix}$	$\begin{pmatrix} 1.14 & 0.44 & 0.35 & 0.0 & 0.0 & 0.0 \\ & 1.32 & 0.38 & 0.0 & 0.0 & 0.0 \\ & & 25.59 & 0.0 & 0.0 & 0.0 \\ & & & 0.35 & 0.0 & 0.0 \\ & & \mathrm{sym} & & 0.13 & 0.0 \\ & & & & & 0.17 \end{pmatrix}$

Tab. 2: The compliance matrix S and the elastic constant matrix C for systems (b) and (c) for model II. Here, we used the relation $C = S^{-1}$ to compute the elasticity matrix C from the matrix S.

System	Model	$E_{33}[\mathrm{GPa}]$	$\nu_{11,33}$	$\nu_{22,33}$	$E_{11}[\mathrm{GPa}]$
(a)	I	0.6142	0.4850	0.4304	0.7100
(a)	II	0.8495	0.4394	0.4501	1.1034
(b)	I	1.4777	0.2778	0.3532	0.6455
(b)	II	1.7422	0.3722	0.3215	0.8043
(c)	I	23.395	0.2161	0.2795	1.1010
(c)	II	25.435	0.2222	0.2157	0.9868

Tab. 3: Elastic moduli and Poisson ratios of the studied systems for model I and model II. Subjected to *transverse* loading conditions, the Young modulus of the composite is in the range of the modulus of the matrix. Subjected to *longitudinal* loading conditions, we see a modulus two times higher for (b) and approximately thirty times higher for (c). For (c) the ROM gives a prediction of $E_{\mathrm{composite}} \approx 27\,\mathrm{GPa}$ for model I and II. There is only a slight difference between model I and II, because no forming or breaking of bonds takes place in these tensile simulations.

4 Concluding Remarks

The macroscopic rule-of-mixtures (*ROM*)

$$E_{\mathrm{composite}} = \Omega_{\mathrm{fiber}} E_{\mathrm{fiber}} + (1 - \Omega_{\mathrm{fiber}}) E_{\mathrm{matrix}} \qquad (8)$$

holds for the long continuous nanotube, but fails for the short fully embedded nanotube; see table 3. The simulation results suggest the possibility to use nanotubes to reinforce an appropriate matrix. They furthermore indicate that long nanotubes should be used. For a fixed tensile loading direction, the nanotubes should be aligned parallel with the loading direction. For general kinds of loading directions, very long nanotubes in random orientation will most likely produce the best results.

5 Acknowledgments

This work was supported by a grant from the *SFB 408* of the *Deutsche Forschungsgemeinschaft*.

References

[1] S. Iijima. Helical microtubules of graphitic carbon. *Nature*, 354:56–58, 1991.

[2] M. M. J. Treacy, T. W. Ebbesen, and J. M. Gibson. Exceptionally high Young's modulus observed for individual carbon nanotubes. *Nature*, 381: 678–680, 1996.

[3] S. J. V. Frankland, A. Caglar, D. W. Brenner, and M. Griebel. Molecular simulation of the influence of chemical cross-links on the shear strength of carbon nanotube-polymer interfaces. *J. Phys. Chem. B*, 106:3046–3048, 2002.

[4] S. J. V. Frankland, V. M. Harik, G. M. Odegard, D. W. Brenner, and T. S. Gates. The stress-strain behavior of polymer-nanotube composites from molecular dynamics simulations. NASA/CR-2002-211953, ICASE Report No. 2002-41, 2002.

[5] S. Nose and M. L. Klein. Constant pressure molecular dynamics for molecular systems. *J. Mol. Phys.*, 50:1055–1076, 1983.

[6] M. Parrinello and R. Rahman. Crystal structure and pair potentials: A molecular-dynamics study. *Phys. Rev. Lett.*, 45(14):1196–1199, 1980.

[7] D. W. Brenner. Empirical potential for hydrocarbons for use in simulating the chemical vapor deposition of diamond films. *Phys. Rev. B*, 42(15): 9458–9471, 1990.

[8] Z. Mao, A. Garg, and S. B. Sinnott. Molecular dynamics simulations of the filling and decorating of carbon nanotubules. *Nanotechnology*, 10:273–277, 1999.

[9] S. H. Lee, H. Lee, H. Pak, and J. C. Rasaiah. Molecular dynamics simulation of liquid alkanes. I. Thermodynamics and structures of normal alkanes: n-butane to n-heptadecane. *Bull. Korean Chem. Soc.*, 17:735–744, 1996.

[10] M. Griebel, A. Caglar, S. Knapek, and G. Zumbusch. *Numerische Simulation in der Moleküldynamik. Numerik, Algorithmen, Parallelisierung, Anwendungen*. Springer, Berlin, Heidelberg, 2003.

[11] D. Beeman. Some multistep methods for use in molecular dynamics calculations. *J. Comp. Phys.*, 20:130–139, 1976.

[12] K. Refson. Molecular dynamics simulation of solid n-butane. *Physica B*, 131:256–266, 1985.